Silicon (2022) 14:6205–6218
https://doi.org/10.1007/s12633-021-01416-6

ORIGINAL PAPER

Investigation of N + SiGe Gate Stacked V-TFET Based on Dopingless Charge Plasma for Gas Sensing Application

Shailendra Singh[1] · Archana Verma[2] · Jeetendra Singh[3] · Girish Wadhwa[4]

Received: 23 August 2021 / Accepted: 20 September 2021 / Published online: 26 September 2021

Abstract

In this paper, a novel n + SiGe pocket layer gate stacked VTFET doping less charge plasma is proposed and analyzed using Silvaco TCAD simulation software. The proposed device will be worked as a transducer sensor which is based upon the principle of the electrostatic charge plasma. The inclusion of doping less charge plasma will ease the device in terms of cost production and form random dopant fluctuation (RDF). The inclusion of charge plasma with gate stacking will enhance the electrostatics control over the gate in order to gain the variation of drain current to boost the current sensitivity. The selection width of the High-K dielectric constant material with SiO_2 will filter out using equivalent gate oxide thickness. The physics behind the change is work function of the gate material in the presence of the gas material is the dissociation and absorption of gas molecule via diffusion process to the catalytic gate metal of the device. In addition, n + SiGe pocket layer is introducing to suppress the tunneling barrier at source channel interface due to reduction in the band gap energy material from 1.1 to 0.7 eV. This paper analysis with oxygen and ammonia gases forms different introduced gate metal electrode such as Silver (m_1 = 4.26–4.46 eV), Molybdenum (m_2 = 4.40–4.60 eV), Ruthenium (m_3 = 4.71–4.91 eV), and Cobalt (m_4 = 5.0–5.20 eV). In this regard, the current sensitivity, electric filed, surface potential, energy band gap and other electrical characteristics with different drain and gate bias with suitable range is operated. The vertical distribution of the channel concentration will improve the device scalability. To test changes in device sensitivity of the catalytic material of the gate electrode will increases as a work function with the range of 50, 100, 150, 200, and 250 meV. The reported sensitivity (I_{don}/I_{doff}) is higher for lower work function i.e. for Silver, Cobalt, Molybdenum and Ruthenium the sensitivity is 4.18×10^2, 3.49×10^2, 1.02×10^3 and 2.79×10^1 respectively.

Keywords Doping less charge plasma vertical tunnel field effect transistor (DCP-VTFET) · Silicon germanium (SiGe) · Subthreshold slope (SS) · BTBT (band to band tunneling) · Gas sensing · Gate stacking

1 Introduction

Over a past decades, continuous down scaling of the CMOS transistor has aggressive improvement in order to enhance the device performance and density [1, 2]. According, to the Moore's law, the device density per unit area will get double in every 18 months [3]. However, after a limit a series issue of the short channel effect will arise and cause in degradation in device performance with the subthreshold slope (SS) limit to 60 mV/dec [4, 5]. Therefore, we need to look beyond the CMOS technology which overcome the limitation of Sub-threshold and short channel effect. According to the ITRS (International Technology Roadmap for Semiconductors), the new roadmap technology for scaling the device channel width, is working with many new devices, among which the TFET technology comes out with ease of fabrication and a potential candidate to overcome the issue of short channel effect [6–9]. The TFET consist of p-i-n structure based on band to band tunneling mechanism, which easily come up with drawback of the leakage current [10, 11]. However, the TFET comes with the own disadvantage of ambipolar conduction which can be engineered by different method [12–14]. In this paper, the detection of gas molecules in low concentration will analyzed when it comes with the contact to gate metal electrode and worked as a gas sensing application in various field like bio-medical, refinery, green energy and

✉ Shailendra Singh
shailendras.nitj@gmail.com

[1] ECE, PSIT Kanpur, Bhautipratappur, India

[2] EL, REC Kannauj, Aher, India

[3] ECE, NIT Sikkim, Sikkim, India

[4] ECE, NIT Jalandhar, Jalandhar, India

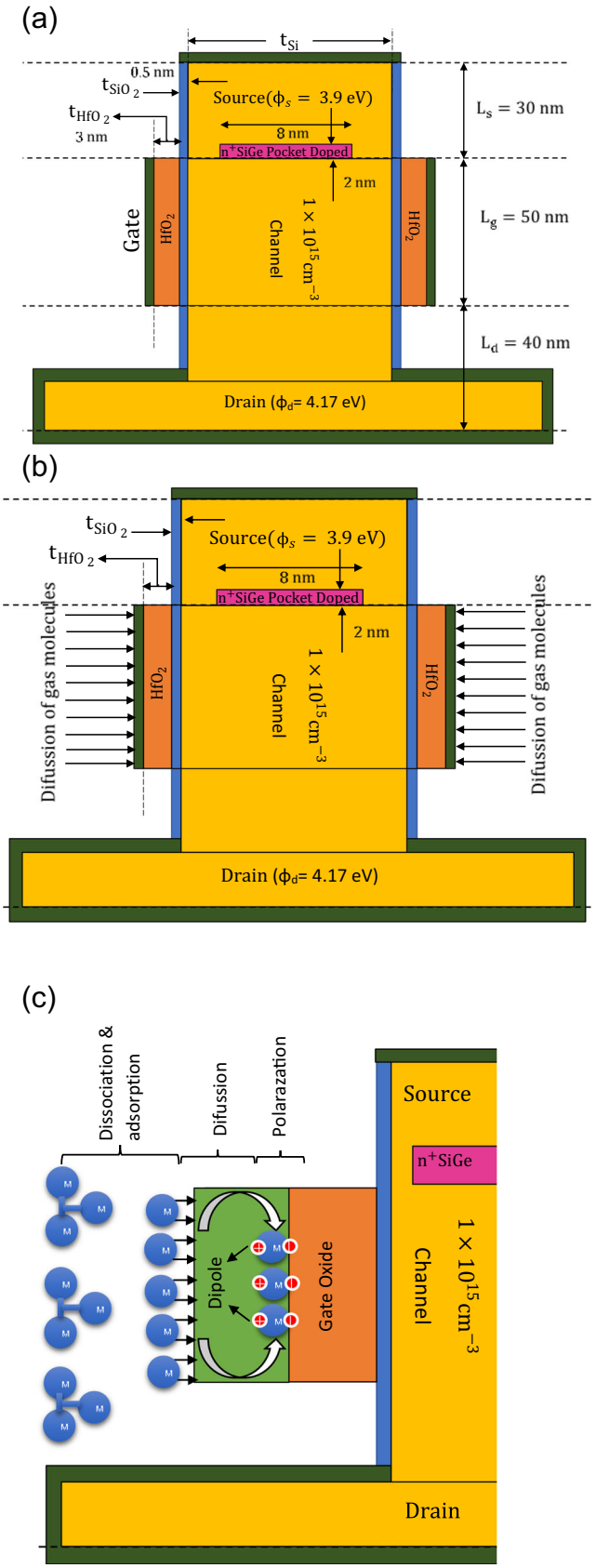

◀ **Fig.1** **a** Schematic diagram of a simulated n + SiGe delta doped gate stacked doping less charge plasma vertical tunnel field transistor (n + SiGe gate staked DCP-VTFET). Figure 1 (**b**) Proposed device with the expose of the gas on the gate metal electrode Fig. 1 **c** Absorption, diffusion and polarised mechanism of gas molecule to the gate electrode medium

environment monitoring for public safety issues. In the regards, the MOSFET already worked as a possible sensor device to develop the reliable gate metal electrode to react with the gas molecules and show the high current sensitivity [15, 16]. This sensor also shows its easy scope of fabrication on chip, scalability and portability. However, it is interesting to note that, with reduce size, TFET bases gas sensor reporting to be a most promising alterative to the conventional MOSFET [17–19]. This superiority over the MOSFET will counterparts due the its working principle of BTBT for the tunneling mechanism [20–22]. In order to determine the performance of any gas sensor, the primary device design working as a transducer matter. Although, many of the device design of MOSFET as an electrochemical gas sensor has been introduce in the past [23, 24]. Now with different working principal of TFET, a new set of design strategies need to be followed. However, as per the literature review, not much of the TFET transduces have been introduced to the system as a gas sensor.

In the era of nanoscale regime, the inclusion of high doping concentration is a challenging issue due to which the problem of random doping fluctuation arises and the cost of the devices will increase [25, 26]. Furthermore, in order to deposit the doped layer, one must involve expensive deposition process such as ion-implantation [27]. On the other hand, a new transistor design-based charge plasma draws special attention that employ a balancing work function at source and drain side to introduce the huge charge carriers in the form of hole and electron respectively. Unlike to the conventional TFET, it has a dopingless channel (1×10^{15} cm^{-3}) with non-metallurgical junction with unform doping at source, channel and drain. The gate metal electrode employed with suitable work function to make the device working as a transducer which also suitable for the label-free bio-sensing applications.

In this paper, a novel n + SiGe pocket layer introduced at source-channel interface, in order to reduce the tunneling barrier for 1.1 eV to 0.7 eV by optimizing the mole fraction at $Si_{1-x}Ge_x$ x = 0.8. The proposed device design of n + SiGe Gate Stacked V-TFET based dopingless charge plasma has significantly show the performance improvement for sensing ammonia and oxygen gases in comparison to the conventional TFET designs using TCAD simulation software [28]. This can be incorporated by employing suitable metal electrodes at the source side and gate side to induce positive charge plasma and which electrostatically improves the gate control over the channel. Even this technology does not the affect the trap assisted tunneling (TAT) parameters of the TFET

Table 1 Selected device design specification of n + sige gate staked dcp-vtfet

Parameter Used	Specification (n+SiGe DCP-VTFET)
Silicon substrate doping (N_d)	1×10^{15} cm^{-3}
N+ SiGe pocket layer doping	1×10^{15} cm^{-3}
Gate Oxide thickness- SiO_2/ HfO_2	0.5 nm/ 3 nm
SiGe layer width	2 nm/8 nm
Body thickness (t_{si})	10 nm
Channel Length (L_g)	50 nm
Source side work function	3.9 eV
Drain side work function	4.17 eV
V_{gs}/V_{ds} operating voltage	1 V/1 V
Total Silicon Substrate length	120 nm

models [29]. As the TAT, known to be degrading the performance of subthreshold regime and affect the current sensitivity. Subsequently, the uniform doping distribution in the direction of tunneling will results in enhanced electrical properties with reduce effect of short channel due to absence of heavy doping gradients. The gate stake method is used to provide better electrostatic control of gate electrode over the channel by inclusion of equivalent oxide thickness. This can be done by introducing the high-k dielectric constant material like HfO_2 (3 nm) with SiO_2 (0.5 nm) in between the channel and gate electrode. The SiO_2 will have adhesive boing with the Silicon wafer and this over-come the problem of the lattice mismatch. The lack of abrupt and abnormal junctions' source-channel and drain, when the doping concentration gradient element is eliminated further simplifies the design of n + SiGe CPD-VTFETs over traditional TFETs.

2 Device Design and Simulation Setup

This schematic diagram of a simulated n + SiGe delta doped gate stacked doping less charge plasma vertical tunnel field transistor (n + SiGe gate staked DCP-VTFET) has been shown in Fig. 1a. A vertical silicon body of uniform doping of 1×10^{15} cm^{-3} with non-metallurgical junction at source, channel and drain is introduced to this paper. The channel length of the device is 50 nm (L_g) with the width of 10 nm (t_{si}) as shown in Table 1. The double gated Vertical TFET structure considers with gate stacked method with high-k (HfO_2) with SiO_2 to avoid lattice mismatch during channel to gate oxide formation. It also enhances the electrostatics gate control over the device channel with control the carrier transport mechanism. The optimized mole fraction for the $Si_{1-x}Ge_x$ material was determined to be x = 0.8, implying that 80% of the germanium percentage was taken at the source-channel interface. As a result, the tunneling barrier will drop from 1.1 to 0.7 eV, improving the device's overall drain current and sensitivity [30]. For both the gate-source (V_{gs}) and drain-source voltages (V_{ds}), the operating voltage of the unit is assumed to be 1 V. Furthermore, this paper discusses oxygen and ammonia gas sensing as shown in Fig. 1b, which will be diffused at gate metal electrode for different materials as per their work function respectively. This can be achieved by

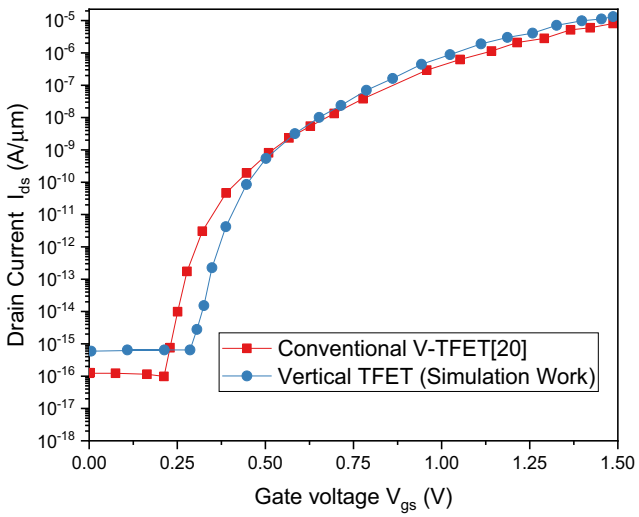

Fig. 2 Calibrated graph against experimental data of vertical TFET with conventional device

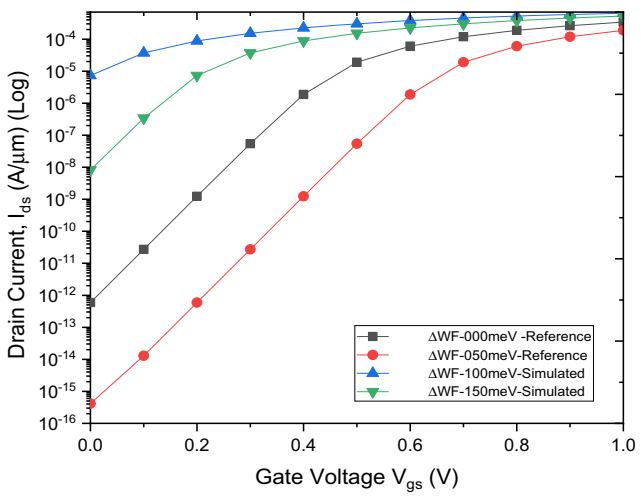

Fig. 3 Comparison of drain characteristics for the metal Molybdenum as a gate metal electrode of proposed device with reference work

Table 2 Sensitivity calculation for silver gate electrode for sensing oxygen gas

$\Delta\phi_M(eV)$	I_{doff}(A/μm)	I_{don}(A/μm)	I_{don}/I_{doff}	S_{doff}
Without Gas	6.42E-07	0.00012145	189.134	1.00E+00
50	1.45E-07	0.000116255	803.399	4.44E+00
100	3.15E-08	0.000111075	3528.79	2.04E+01
150	6.89E-09	0.000105933	15,380.9	9.32E+01
200	1.54E-09	0.000100834	65,685.6	4.18E+02

Table 4 Sensitivity calculation for ruthenium gate electrode for sensing ammonia gas

$\Delta\phi_M(eV)$	I_{doff}(A/μm)	I_{don}(A/μm)	I_{don}/I_{doff}	S_{doff}
Without Gas	1.40E-12	7.58E-05	5.42E+07	1.00E+00
50	2.92E-13	7.07E-05	2.42E+08	4.79E+00
100	4.95E-14	6.56E-05	1.33E+09	2.83E+01
150	8.26E-15	6.05E-05	7.33E+09	1.70E+02
200	1.38E-15	5.54E-05	4.02E+10	1.02E+03

using high reactive metals as gate metals, such as Silver (m_1 = 4.26–4.46 eV), Molybdenum (m_2 = 4.40–4.60 eV), Ruthenium (m_3 = 4.71–4.91 eV), and Cobalt (m_4 = 5.0–5.20 eV). Now, Fig. 1c show the dissociation and the absorption of the gas molecule at the surface of gate metal electrode, which further gets polarized and make the dipole at the dielectric oxide interface and stick to it. Subsequently, this will charge induce to the channel i.e. equivalent to the change in work function, which increases the current sensitivity and enhance the device for gas sensing application. To build the source side as p-type junction one has to raise the contact magnitude of metal work function. The main purpose is to make the device working as p-i-n structure instead of n+/n+/n + structure. To make the junction virtually, one has to optimized the work function in order to induce the source-drain junction. Employing a suitable work function of metal electrodes, a source "p" and drain "n" are developed on an intrinsic body in charge plasma technique. This method evenly distributes electron concentrations at the source/drain electrode's top and bottom, allowing for improved control in order to enhance device ON-current. To increase the majority of p-type charge carries, we need to do additional biasing at the source side. Due to this, there will be a rise in power consumption, which is a major problem with the electrostatic technique. Fabrication of charge Plasma devices necessitates an additional metallization process stage because of the requirement for metal electrode to vary with work functions. An intrinsic body is employed to establish a source-drain section and a doping-free structure using electrostatically charged plasma. On the side of source, the n type region is created by choosing the required work property of the metal electrode, and on the side of drain, the n type region is created by applying bias to the metal electrode using the charge plasma technique. At the drain side, an electrostatic technique is used; the drain side polarity gate with applied V_{ds} is made of metal deposited over an oxide layer. As a result, compared to individual dopingless methods, the fabrication process becomes more straightforward. On the source side, a charge plasma method is used to produce n type doping in the source by using the right work function metal for the source metal. As a result, additional source biasing is not needed and the total amount of power consumption decreased.

TCAD Silvaco simulation software is used to drive the electrical characteristics in order to find out the gas sensitivity parameters. To include the physics of carrier transport, the drift diffusion model is used. The fermi-dirac, band gap narrowing model and the low electric field dependent mobility concentration model are also incorporated. The phonon-assist dynamic nonlocal band to band tunneling is employed for computing the tunneling path form energy band profile. The Schottky-read-Hall (SRH) recombination and Trap-assisted Tunneling (TAT) are used for optimizing the effect of quantum tunneling and being used to investigate the doping and temperature effect. The proposed system is tested using VTFET experimental data, as shown in Fig. 2, and data about the channel present is obtained using the Plot Digitizer process.

3 Structure Validation with Reference Structure

The vertical dual gate structure provides greater gate control than conventional designs for band-to-band tunneling (BTBT). This

Table 3 Sensitivity calculation for molybdenum gate electrode for sensing ammonia gas

$\Delta\phi_M(eV)$	I_{doff}(A/μm)	I_{don}(A/μm)	I_{don}/I_{doff}	S_{doff}
Without Gas	9.32E-09	0.000106958	11,474.2	1.00E+00
50	2.07E-09	0.00010185	49,228.8	4.50E+00
100	4.70E-10	9.68E-05	2.06E+05	1.98E+01
150	1.10E-10	9.18E-05	8.34E+05	8.47E+01
200	2.67E-11	8.68E-05	3.25E+06	3.49E+02

Table 5 Sensitivity calculation for cobalt gate electrode for sensing ammonia gas

$\Delta\phi_M(eV)$	I_{doff}(A/μm)	I_{don}(A/μm)	I_{don}/I_{doff}	S_{doff}
Without Gas	5.67E-17	4.60E-05	8.12E+11	1.00E+00
50	1.11E-17	4.06E-05	3.65E+12	5.10E+00
100	3.54E-18	3.50E-05	9.89E+12	1.60E+01
150	2.27E-18	2.91E-05	1.28E+13	2.50E+01
200	2.03E-18	2.26E-05	1.11E+13	2.79E+01

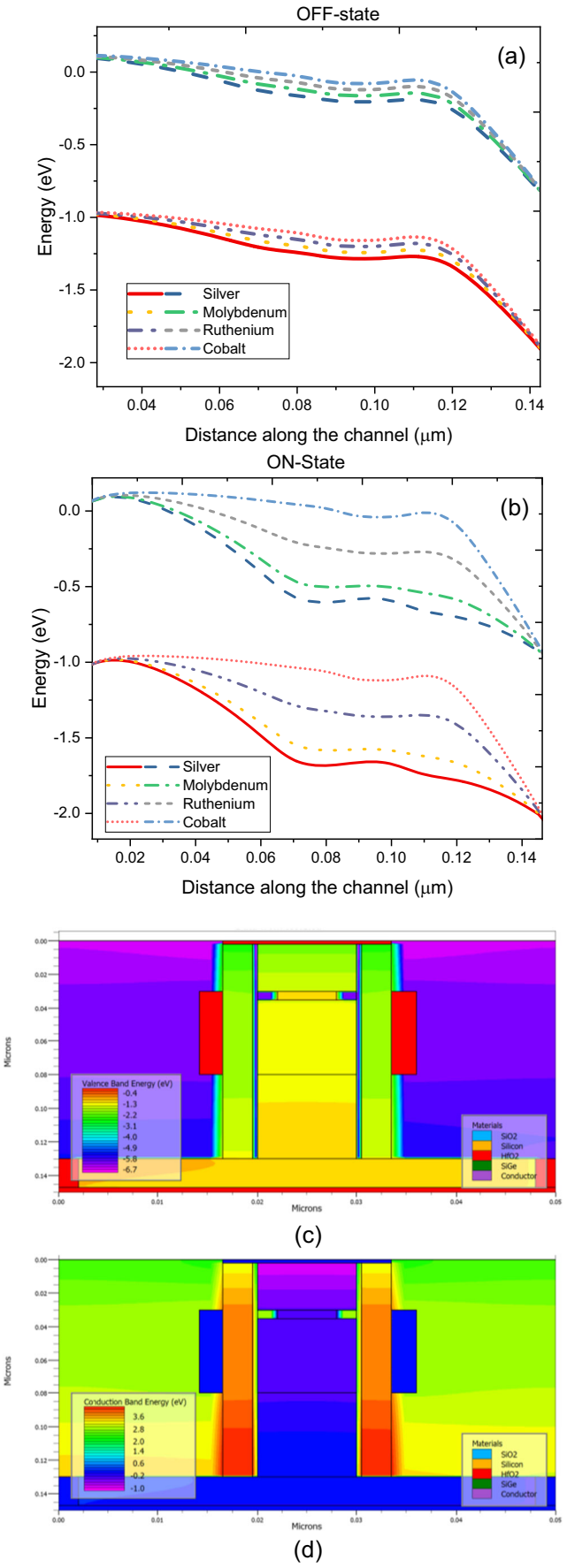

◀ **Fig. 4** Energy band diagram of valance band and conduction band (**a**) OFF-state and (**b**) ON-state with 2D contour plots of (**c**) valence band energy distribution (**d**) conduction band energy distribution of n + SiGe gate staked DCP-VTFET with respect to different metal Silver, Molybdenum, Ruthenium &Cobalt at Vgs = 1 V and Vds = 1 V

suggested device could be used for gas sensing in a variety of applications because of its low subthreshold slope (SS) and high ON-state current. The use of gate metal as a Molybdenum catalyst contact in N+ SiGe pocket gate stacked DCP-VTFETs with ammonia sensing is investigated. The ON-state current in Fig. 3 is extremely high as compared to the cited structure. The sensitivity values for Dopingless CP-VTFET based sensors using Co, Mo, and Pd metals as gate contacts are much higher than earlier gas sensor designs (The calculations for sensitivity are given in Tables 2, 3, 4, and 5).

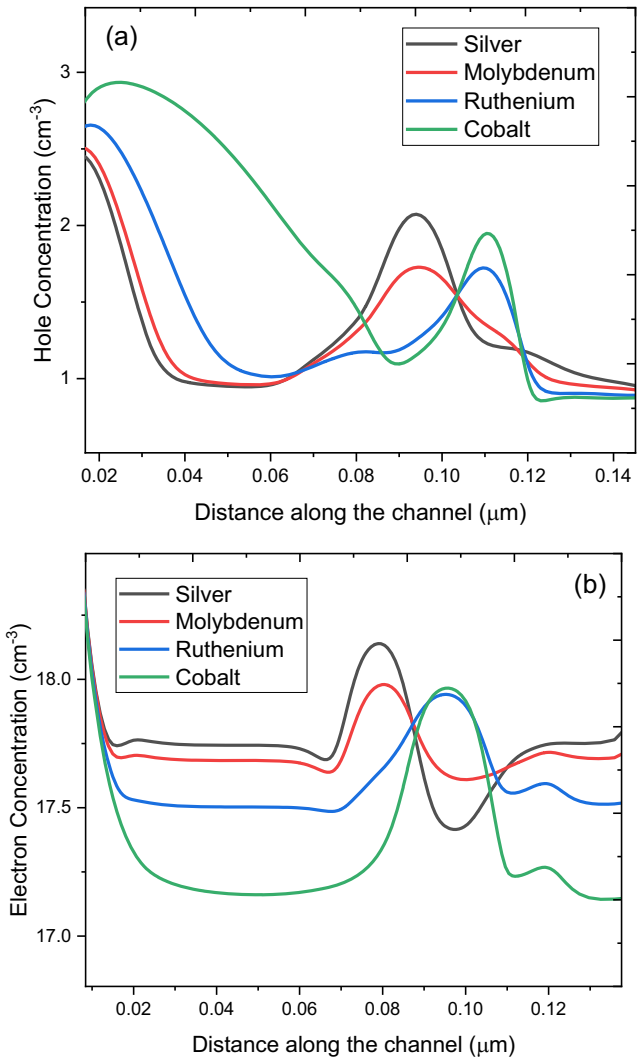

Fig. 5 **a** Electron Concentration and **b** Hole Concentration of n + SiGe gate staked DCP-VTFET with respect to to different gate electrode Silver, Molybdenum, Ruthenium &Cobalt at Vgs = 1 V and Vds = 1 V

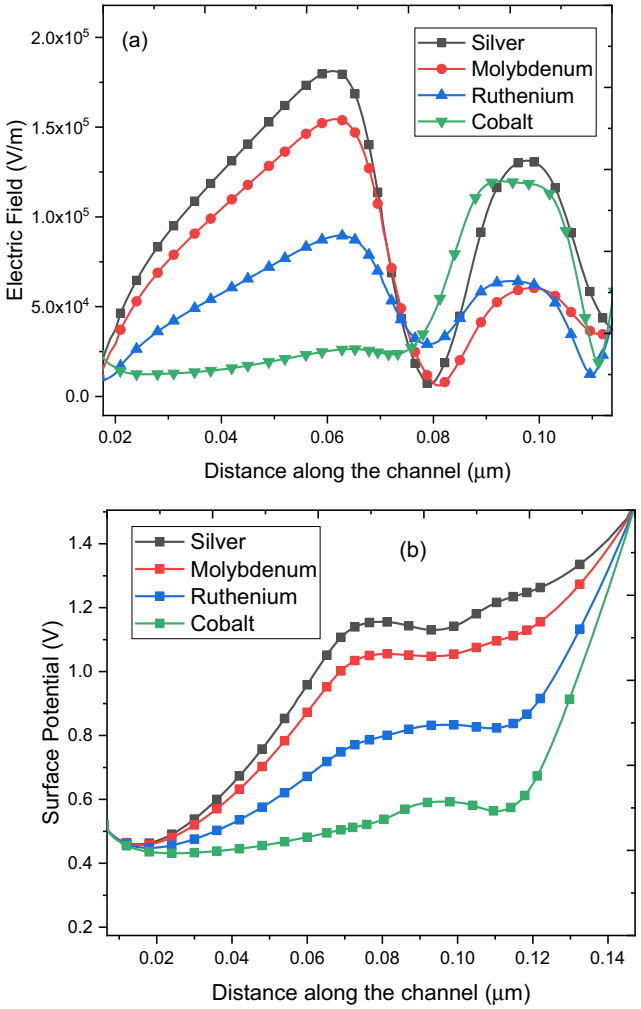

Fig. 6 **a** Electric field **b** channel potential of n + SiGe gate staked DCP-VTFET with respect to to different gate electrode Silver, Molybdenum, Ruthenium &Cobalt at Vgs = 1 V and Vds = 1 V

4 Device Simulation and its Electrical Characteristics

In order to understand the physics behind the proposed structure one has to study the derived electrical characteristics like its energy band diagram, electric field, surface potential and electron and hole concentration with respect to the channel position.

The proposed device's conduction and valence energy band are seen in Fig. 4a for the OFF-state region. Since the cobalt have the highest work function than Ruthenium, Molybdenum and Silver, so its band shift is highest than other due to the higher concentration, which will induce a greater number of charge carriers in the source side region. Now Fig. 4b show the energy band diagram of the ON-state, in which the Positive biasing causes the energy band to transfer down form the drain side which cause the higher drain current due to electron drift form source to drain side. Higher applied voltage in the drain side will induces a greater number of n-type charge carriers, however, the charge plasma produce in the source side will produce a greater number of charges carries than to drain side [31, 32]. Figures 4c and d show a 2D contour diagram of the valence band and conduction band, respectively, from which it can be inferred that energy at the control gate allows electrons to move from the source to the drain field. The graph also shows that as you move closer to the drain, the number of electrons decreases. Similarly, due to the high work function, which is considered p-type in vertical tunneling, holes will accumulate near the source field, and the energy band will be pulled down as the work function increases.

In Fig. 5a and b, we observe the equivalent electron and hole concentration with respect to the channel position. In the channel region the electron having the higher concentrations due to high rate of inversion charge carrier at the form positive polarity gate electrode. As the total device is of n-type, due to higher concentration of electron at the source side due to low work function with the value of 3.9 eV. However, in the spacer region, the electron concentration is low due to the diffusion form source to spacer region. Similarly, in the drain side due positive biasing of the drain voltage the electron concentration is high at the drain-channel interface region. Due to Schottky contact with the drain contact and its semiconductor region, the electron concentration is low because of formation of depletion region [33, 34]. In the next Fig. 5b of the hole concentration with respect to the channel position is less comparatively to drain and the source side. This happen due to the hole's repulsion & lower work function from the drain side in the ON state condition. Among all gate electrode material, cobalt is having the highest work function with the value of 5.0 eV, which repels the p-type charge carriers and makes the hole concentration lowest at the channel region as compares to other metal gate electrode like Ruthenium, Molybdenum and Silver.

Figure 6a shown the large variation of electric field at the tunneling junction after the gas dissociation and absorption in comparison to all other gate electrode metal. The electric field can be observed form the fermi-level gradient across the channel length. At the drain-channel interface the electric field increases due to rise in the energy and become saturated at the gate region due to linear in the Fermi Level. The proportionate variance of the electric field with regard to the work function is shown in Fig. 6a. The greater the value of the electric field reported as the work function increases due to different metal catalysts. This occurs due to a reduction in charge carrier mobility across the channel [35]. The electric field value increases steadily in the drain field, resulting in a constant, slowly decreasing slope in the potential curve [36]. The electric field is depicted as a part of the fermi-Dirac distribution with electron density in this diagram. Subsequently, in Fig. 6b shown the variation of the surface potential of the

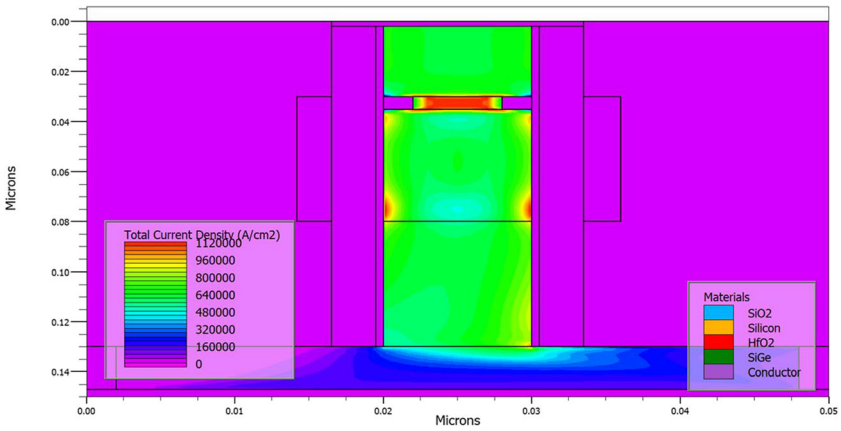

Fig. 7 2D contour plot of electron current density distribution of the n + SiGe gate staked DCP-VTFET proposed device

proposed device. As surface potential, is the negative integral of the electric field. In the drain field, the electric field value gradually increases, resulting in a constant, slowly decreasing slope in the potential curve. Therefore, superiority of the transducer efficiency mainly observes form the electric and potential field of the device.

5 N + SIGE POCKET GATE STACKED DCP-VTFET WORKING AND ITS FEATURE

Gas sensors work by turning gaseous concentrations of various gases into electrical signals through chemical and physical processes. Gases like O_2 and NH_3 bond to the surface of gate

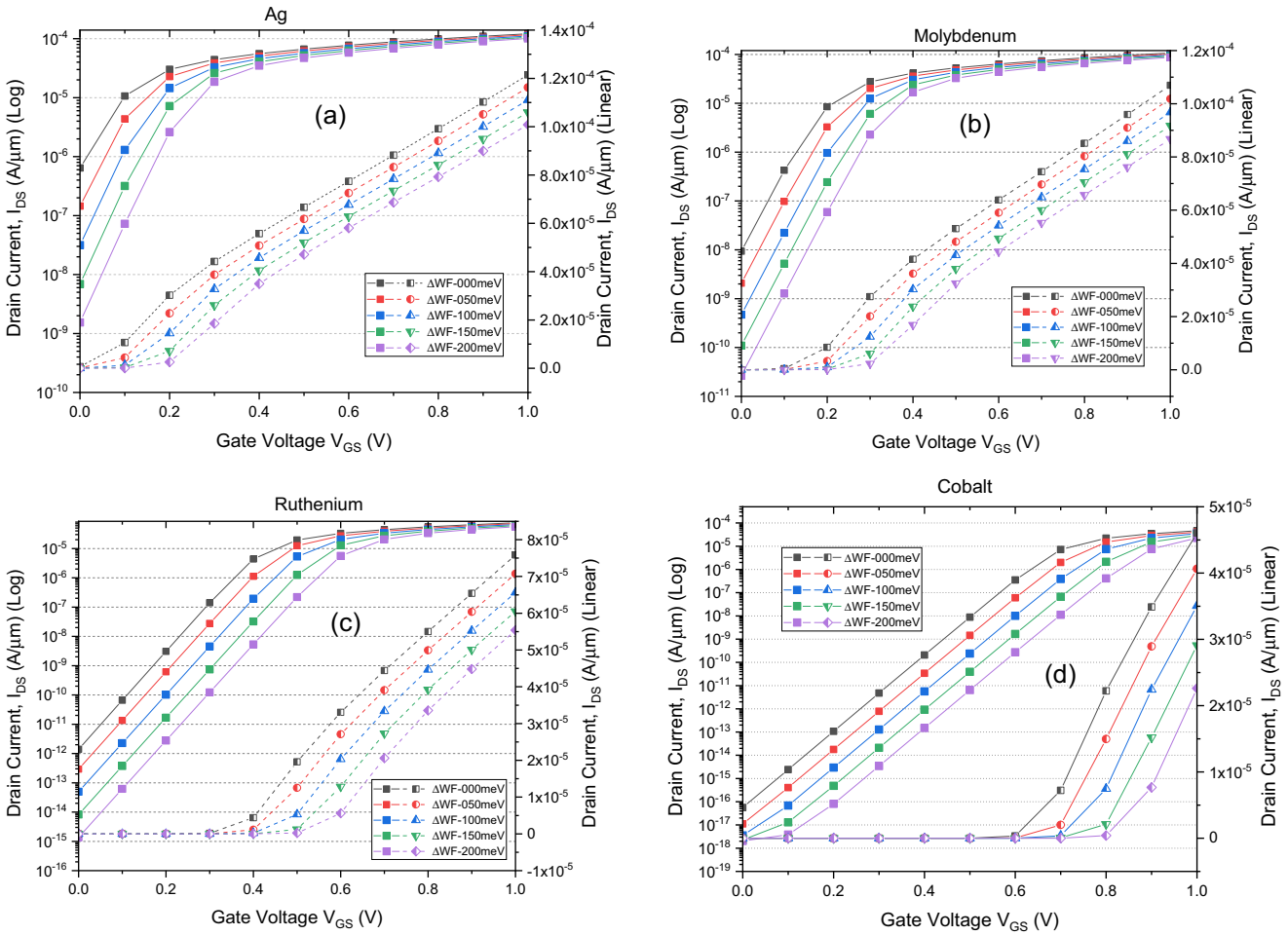

Fig. 8 Variation of drain current characteristics (Idoff) of the n + SiGe gate staked DCP-VTFET with presence and without presence of gas molecules for (**a**) Silver (**b**) Molybdenum (**c**) Ruthenium (**d**) Cobalt

contacts made of catalytic metals, causing the gate's work function to change. Due to harmful gas molecule adsorption, Eq. (1) effects work feature variability.

$$\Delta\phi_m = cont - \left[\left(\frac{RT}{4F}\right) \times ln(P)\right] \quad (1)$$

The gas constant is R, absolute temperature is T, and Faraday's constant and partial pressure are F and P. The relational dependence of a gas's partial pressure on its concentrations can be used to calibrate this system in terms of the gas's mole fractions in the air.

The importance of WFV to V_{fb} is defined by Eq. (2) [37].

$$V_{fb} = \phi_m - \phi_s \pm \Delta\phi_m \quad (2)$$

Where ϕ_s denotes the silicon work function and ϕ_m denotes the metal work function.

However, the delta symbol used $\Delta\phi_m$ is employed to exploit variation in the gate metal work function.

$$\phi_s = \frac{E_g}{2} + \chi - q\phi_{fp} \quad (3)$$

The OFF-state (I_{doff}) current changes proportionately as the subthreshold slope changes, resulting in a change in subthreshold voltage, V_{th}.

$$I_{subthreshold} = I_0\left[e^{\frac{V_{gs}-V_{th}}{\eta V_{th}}}\right]\left[1 - e^{\frac{-V_{ds}}{V_{th}}}\right] \quad (4)$$

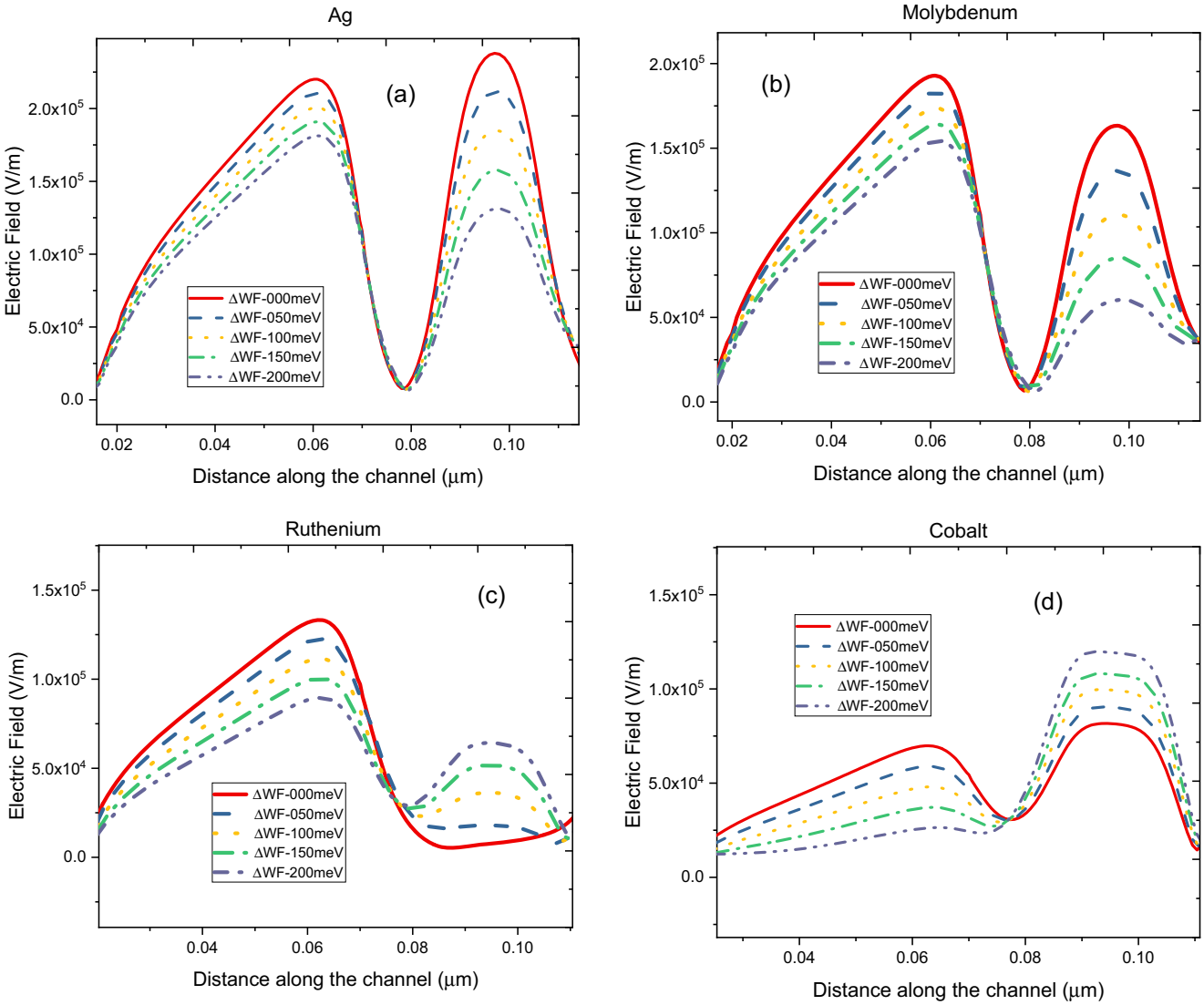

Fig. 9 Variation of electric field characteristics of n + SiGe gate staked DCP-VTFET with presence and without presence of gas molecules for (**a**) Silver (**b**) Molybdenum (**c**) Ruthenium (**d**) Cobalt

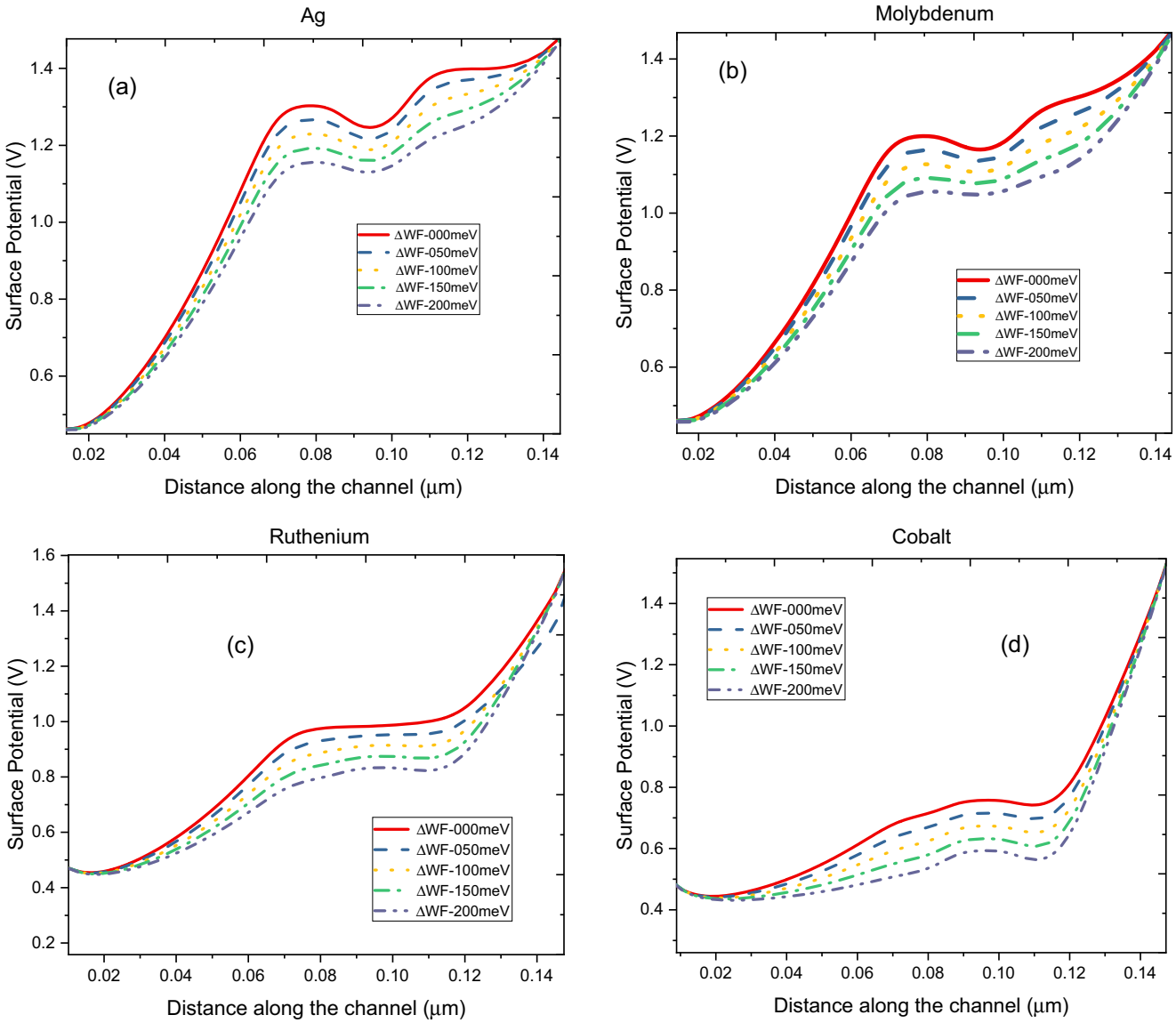

Fig. 10 Variation of surface potential characteristics of n + SiGe gate staked DCP-VTFET with presence and without presence of gas molecules for (a) Silver (b) Molybdenum (c) Ruthenium (d) Cobalt

Where,

$$I_o = \frac{w\mu_n C_{ox} V_T^2 e^{1.8}}{L} V_T \tag{5}$$

The operational voltages of the device are represented by V_{gs}, V_{ds}, and V_T, which stand for gate-source voltage, drain-source voltage, and thermal voltage, respectively. The effective width and length of a transistor are indicated by L and w, respectively. C_{ox} stands for gate oxide capacitance, μ_n for electron mobility, and η for subthreshold swing coefficient. As a result, the relationships between work function variation, threshold voltage (V_{th}), and transistor currents are defined by the equations above.

The suggested DCP-VTFET's conduction behavior is investigated using surface potential, electric field, and energy band characteristics curves. The electrostatic potential rises as the electron current density near the source-channel contact rises, as seen in Fig. 7, which represent the equivalent 2D contour plot o electron current density. This is owing to the gate metal electrode's great electrostatic control over the channel.

In order to drive the drain current, one have used the proposed device of the n + SiGe gate staked DCP-VTFET as a transducer. The reaction of gaseous molecules to the metallic surface will employed the electric variation in terms of variation in the I_{doff} current [38]. We investigated the effect of changing the WFV from the reference value of the metallic work function catalyst by applying 50, 100, 150, and 200 meV to the drain current of Silver, Molybdenum,

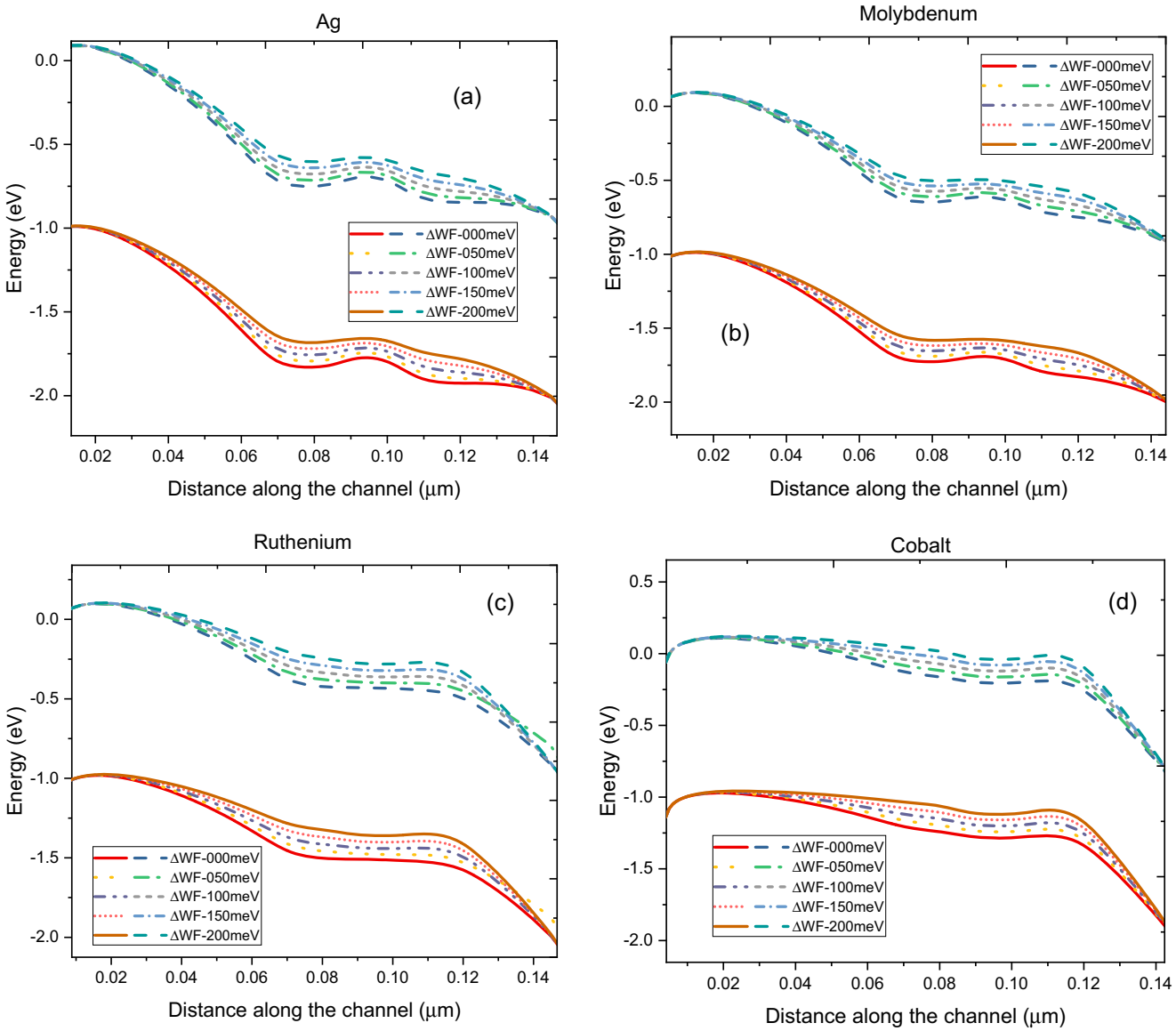

Fig. 11 Variation of energy band diagram characteristics of n + SiGe gate staked DCP-VTFET with presence and without presence of gas molecules for (**a**) Silver (**b**) Molybdenum (**c**) Ruthenium (**d**) Cobalt

Ruthenium and Cobalt respectively. It can be shown in Fig. 8a, b, c, and d that the OFF-state current varies greatly when compared to the ON-state current. As a result, decreasing the OFF current exponentially increases the sensitivity in the subthreshold zone, as shown by Eq. (6).

$$S_{Idoff} = \frac{I_{doff\,(without\ gas)}}{Idoff_{\,(with\ gas)}} \tag{6}$$

Furthermore, because Vertical TFET are less resistant to the work function of the metal electrodes, variations in the workfunction will cause changes in the subthreshold voltage. (Tables 2, 3, 4, and 5 show the sensitivity calculations.

6 N + SIGE POCKET GATE STACKED DCP-VTFET PERFORMANCE ANALYSIS AND COMPARISON

In this section, the sensitivity changes observed in terms of electric field, surface potential and energy band diagram for the different catalytic metal as a gate electrode like Silver, Molybdenum, Ruthenium and cobalt for sensing oxygen and ammonia gases.

For the catalyst metals gate electrode like Silver, Molybdenum, Ruthenium and cobalt respectively, Figs. 9 and 10 depicts the combined electric field and surface potential with respect to the WFV. The electric field is directly proportional to the work function value, as seen in the figure;

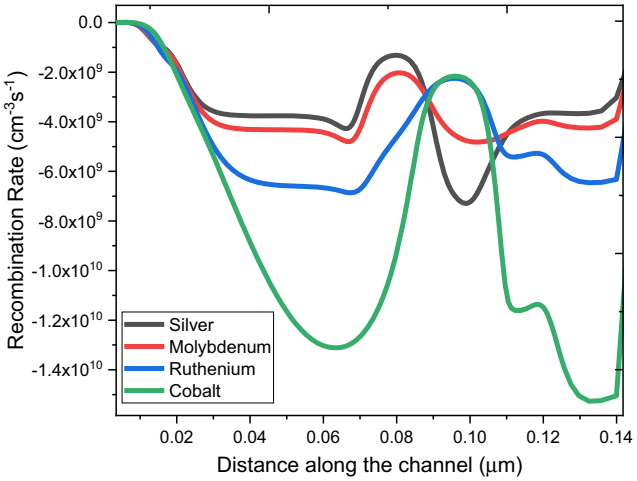

Fig. 12 Analysis of recombination rate of n + SiGe Gate stacked DCP-VTFET at Vgs = 1 V and Vds = 1 V

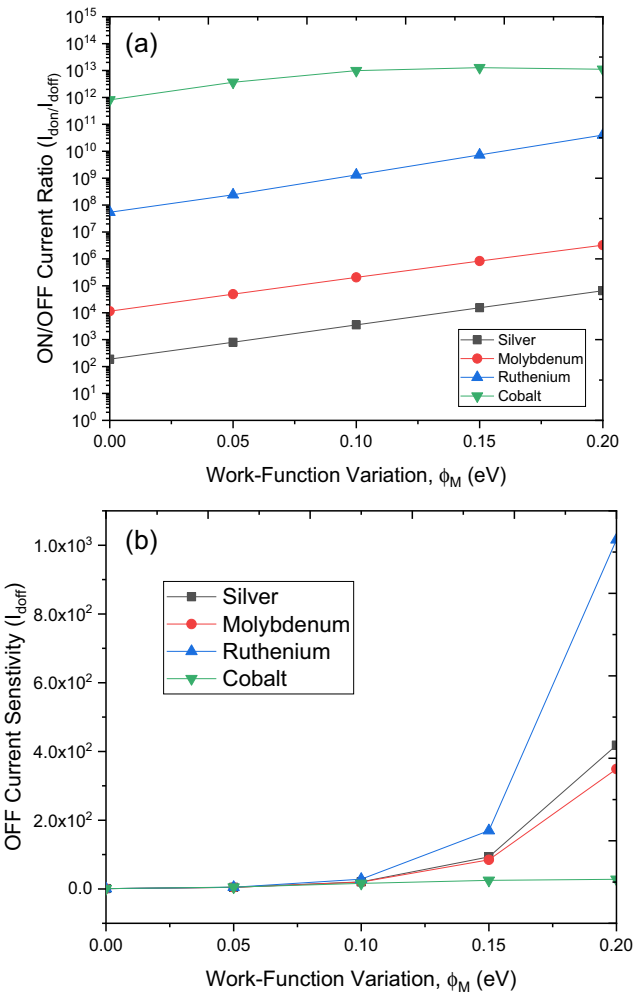

Fig. 13 Variation of (**a**) ON/OFF current (**b**) OFF current sensitivity (SIdoff) of of n + SiGe Gate stacked DCP-VTFET at Vgs = 1 V and Vds = 1 V

as the WFV increases, the electric field increases as well. It has sharp edges at the source-channel interface due to the presence of a delta-doping layer, which increases fee transmission by lowering the band gap at the tunneling junction.

As a result, the variance of the surface potential in Fig. 10a, b, c, and d would appear to have a slightly inverse relationship to the WFV. This occurs because the majority of charge carriers change their state to p-type, posing a barrier to tunnelling current and lowering the surface potential overall. As we move the length of the device, the electric field reaches its maximum value across the channel. As a result, the surface potential is defined as the electric field's negative integral.

The evolution of energy band diagrams as the work function increases is depicted in Figs. 11a, b, c, and d. Cobalt has the highest tunneling barrier (Fig. 5a) since the work feature at the gate electrode is the highest. Furthermore, extra n-type charge carries are drawn to the drain-side due to a higher drain bias. In Fig. 4b, the cumulative effect is shown as individual peak formation for each gate-metal-electrode. The higher work mechanism causes a higher concentration of p-type to form, which is the primary cause of energy band shifts. Due to the higher work function applied to the source-terminal, p + pockets induced near the source-channel interface facilitate more tunneling than those induced near the drain field. As shown in the graphs, increased tunneling begins in an extended bandgap close to the drain region as compared to source-channel space.

7 Result and Discussion

In this section the role of n + SiGe gate staked DCP-VTFET is shown as a transducer. It can be seen from the Fig. 12, that the recombination rate at the source-channel interface is almost nil form the n + SiGe DCP-VTFET due to the negligible minority charge carrier in this region due to the presence of N+ pocket doping.

For Silver, Molybdenum, Ruthenium & Cobalt, Fig. 13a depicts the ON/OFF current ratio with respect to the metal gate electrode. The inverse linear relationship between the variance of a high work function and the current ratio is clearly visible in this graph. As the work function increases in value, the ON/OFF current has a lower ration among them, resulting in an overall decrease. However, for metal Silver, Molybdenum, Ruthenium & Cobalt, Fig. 13b demonstrates the variance of derive sensitivity using Eq. (6) with respect to metal gate electrode. Tables 2, 3, 4, and 5 shows that the derived sensitivity is higher for the lower work function, i.e. is 4.18×10^2, 3.49×10^2, 1.02×10^3 and 2.79×10^1 for Silver, Molybdenum, Ruthenium & Cobalt respectively. Because of the inclusion of the SiGe Layer, the potential barrier at the source-channel interface is less affected. As a result, we can deduce that as the OFF current decreases, the sensitivity increases.

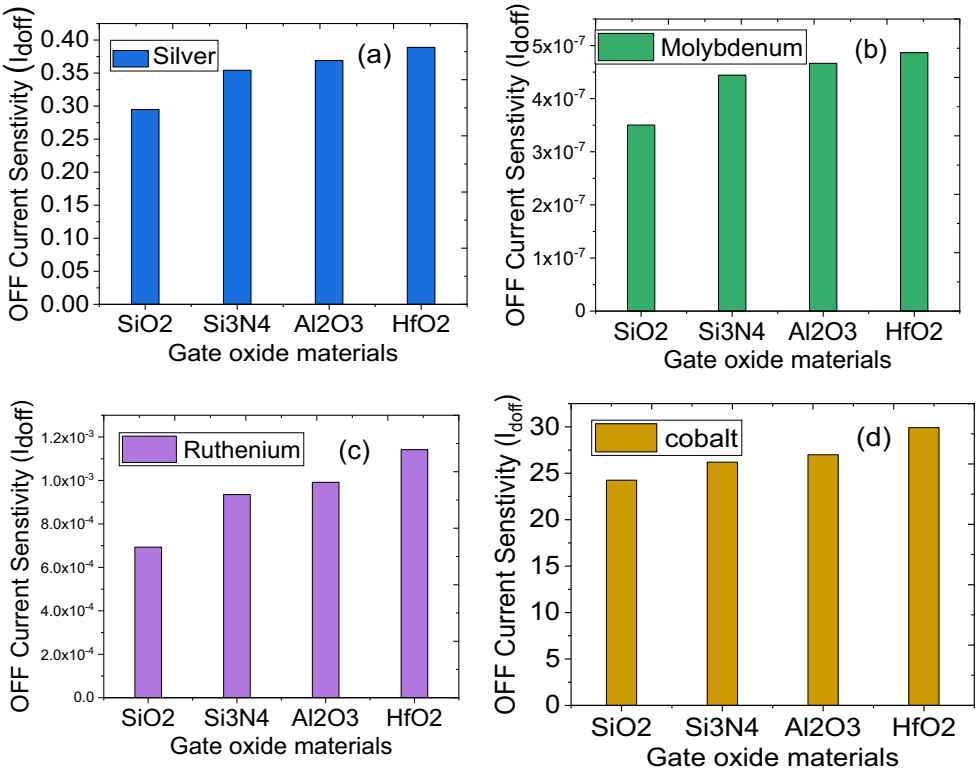

Fig. 14 Variation of different dielectric material of sensitivity for oxygen and ammonia gas for different gate metal electrode (**a**) Silver (**b**) Molybdenum (**c**) Ruthenium (**d**) Cobalt of n + SiGe Gate stacked DCP-VTFET at Vgs = 1 V and Vds = 1 V

Figure 14a, b, c, and d show the variation of different dielectric material using Eq. (7) for different gate electrode with contact catalytic metal for sensing oxygen and ammonia gas as gas sensor.

$$C_{OX} = \frac{2\varepsilon_O \epsilon_{slo_2} L_g}{\ln\left(\frac{rG}{rNW}\right)} \tag{7}$$

Form the above equation its can be predict that, Cox (oxide capacitance) is directly proportional to the dielectric constant magnitude which raise in the ON and OFF current simultaneously. We have taken four different dielectric constants (SiO_2 (3.9), Si_3N_4 (7.5), Al_2O_3 (9.5), HfO_2(21)) with respect to ON/OFF current sensitivity. In this context, we get to know that, higher the dielectric constant value will increase the drain ON current as well as OFF current. The off current variation is responsible for the high current sensitivity and it can be highly varied by the high k-dielectric constant. Therefore, it can be concluded form the figure that, current sensitivity is highest for HfO_2 rather than others.

8 Conclusion

The design and performance of a novel n + SiGe pocket layer gate stacked VTFET doping less charge plasma is analyzed using Silvaco TCAD simulation software. The idea of a double metal gate doping less charge plasma Vertical TFET as a gas sensor with high sensitivity has been applied in the literature. The recorded sensitivity (I_{don}/I_{doff}) is higher for lower work function i.e. for Silver, Cobalt, Molybdenum and Ruthenium the sensitivity is 4.18 × 10^2, 3.49 × 10^2, 1.02 × 10^3 and 2.79 × 10^1 respectively, for a quick enhancement at the value of 200 meV work function, which reflects the efficiency of the proposed structure. The sensitivity of the proposed device has been explored by using different parameters like electric filed, energy band diagram, channel potential, different dielectric material. Result reveals that HfO2 found to be a strong dielectric medium for recording high absorption sensitivity up to 10^{-18} (A/μm) as an OFF current. In future once optimized this device, by engineering the parameters of channel length and dual or triple gate-related design. Therefore, n + SiGe Gate stacked DPC-VTFET proves to be a promising candidate for application as a gas sensor, which can easily helpful in the commercial to estimate the amount of gas present in chemical, medical, automotive industries.

Availability of Data and Material Not applicable.

Author Contributions All authors have equally participated in the preparing of the manuscript during implementation of ideas, findings result, and writing of the manuscript.

Funding The author(s) received no financial support for the research, authorship, and/or publication of this article.

Data Availability Not applicable.

Declarations All procedures performed in studies involving human participants were in accordance with the ethical standards.

Consent to Participate Not applicable.

Consent for Publication The Author transfers his copyrights to the publisher.

Conflict of Interest The authors declare that there are no conflicts of interest.

References

1. Frank DJ, Dennard RH, Nowak E, Solomon PM, Taur Y, Wong H-SP (2001) Device scaling limits of Si MOSFETs and their application dependencies. *Proc. IEEE* 89(3):259–288. https://doi.org/10.1109/5.915374
2. Koswatta SO, Lundstrom MS, Nikonov DE (2009) Performance comparison between pin tunneling transistors and conventional MOSFETs. IEEE Trans. Electron Devices 56(3):456–465. https://doi.org/10.1109/TED.2008.2011934
3. Thompson SE, Parthasarathy S (2006) Moore's law: the future of Si microelectronics. Mater. Today 9(6):20–25
4. Koswatta SO, Koester SJ, Haensch W (2010) On the possibility of obtaining MOSFET-like performance and sub-60-mV/dec swing in 1-D broken-gap tunnel transistors. IEEE Trans. Electron Devices 57(12):3222–3230
5. Singh, S., Raj, B.: Study of parametric variations on hetero-junction vertical t-shape TFET for suppressing ambipolar conduction. (2020)
6. Schaller, R.R.: Technological innovation in the semiconductor industry: a case study of the International Technology Roadmap for Semiconductors (ITRS). PhD diss., George Mason University, (2004)
7. Baxter J, Bian Z, Chen G, Danielson D, Dresselhaus MS, Fedorov AG, Fisher TS et al (2009) Nanoscale design to enable the revolution in renewable energy. Energy Environ. Sci. 2(6):559–588
8. Yang M, Cao K, Sui L, Qi Y, Zhu J, Waas A, Arruda EM, Kieffer J, Thouless MD, Kotov NA (2011) Dispersions of aramid nanofibers: a new nanoscale building block. ACS Nano 5(9):6945–6954
9. Singh, S., Raj, B. Vertical tunnel-fet analysis for excessive low power digital applications. In: 2018 First International Conference on Secure Cyber Computing and Communication (ICSCCC), pp. 192–197. IEEE (2018)
10. Choi WY, Park B-G, Lee JD, Liu T-JK (2007) Tunneling field-effect transistors (TFETs) with subthreshold swing (SS) less than 60 mV/dec. IEEE Electron Device Lett. 28(8):743–745. https://doi.org/10.1109/LED.2007.901273
11. Khatami Y, Banerjee K (2009) Steep Subthreshold Slope n- and p-Type Tunnel-FET Devices for Low-Power and Energy- Efficient Digital Circuits. IEEE Trans. Electron Devices 56(11):2752–2760. https://doi.org/10.1109/TED.2009.2030831
12. Raad B, Nigam K, Sharma D, Kondekar P (2016) Dielectric and work function engineered TFET for ambipolar suppression and RF performance enhancement. Electron. Lett. 52(9):770–772
13. Singh S, Raj B (2020) Two-dimensional analytical modeling of the surface potential and drain current of a double-gate vertical t-shaped tunnel field-effect transistor. J. Comput. Electron. 19(3):1154–1163
14. Singh S, Raj B (2019) Design and analysis of a heterojunction vertical t-shaped tunnel field effect transistor. J. Electron. Mater. 48(10):6253–6260
15. Kim C-H, Cho I-T, Shin J-M, Choi K-B, Lee J-K, Lee J-H (2013) A new gas sensor based on MOSFET having a horizontal floating-gate. IEEE Electron Device Lett. 35(2):265–267
16. Anand S, Singh A, Amin SI, Thool AS (2019) Design and performance analysis of dielectrically modulated doping-less tunnel FET-based label free biosensor. IEEE Sensors J. 19(12):4369–4374
17. Bala S, Khosla M (2018) Design and analysis of electrostatic doped tunnel CNTFET for various process parameters variation. Superlattice. Microst. 124:160–167
18. Som D, Majumdar B, Kundu S, Kanungo S (2020) Investigation of charge plasma-enhanced tunnel field-effect transistor for hydrogen gas sensing application. IEEE Sens. Lett. 4(6):1–4
19. Bala S, Khosla M (2019) Design and performance analysis of low-power SRAM based on electrostatically doped tunnel CNTFETs. J. Comput. Electron. 18(3):856–863
20. Nigam K, Kondekar P, Sharma D (2016) High frequency performance of dual metal gate vertical tunnel field effect transistor based on work function engineering. Micro Nano Lett. 11(6):319–322
21. Singh S, Raj B (2020) Analytical modeling and simulation analysis of T-shaped III-V heterojunction vertical T-FET. Superlattice. Microst. 147:106717
22. Anand S, Amin SI, Sarin RK (2016) Performance analysis of charge plasma based dual electrode tunnel FET. J. Semicond. 37(5):054003
23. Seo H, Endoh T, Fukuda H, Nomura S (1997) Highly sensitive MOSFET gas sensors with porous platinum gate electrode. Electron. Lett. 33(6):535–536
24. Singh S, Raj B (2021) Analytical and compact modeling analysis of a SiGe hetero-material vertical L-shaped TFET. Silicon:1–11
25. Damrongplasit N, Kim SH, Liu T-JK (2013) Study of random dopant fluctuation induced variability in the raised-Ge-source TFET. IEEE Electron Device Lett. 34(2):184–186
26. Singh S, Yadav S, Bhalla SK (2021) An Improved Analytical Modeling and Simulation of Gate Stacked Linearly Graded Work Function Vertical TFET. Silicon:1–14
27. Yoon J-S, Baek R-H (2018) Study on random dopant fluctuation in core–shell tunneling field-effect transistors. IEEE Trans. Electron Devices 65(8):3131–3135
28. Manual, Atlas Users. Device simulation software, Silvaco Int. Santa Clara, CA, Version 5, no. 0 (2010)
29. Vandooren A, Daniele L, Rooyackers R, Hikavyy A, Devriendt K, Demand M, Loo R, Groeseneken G, Huyghebaert C (2013) Analysis of trap-assisted tunneling in vertical Si homo-junction and SiGe hetero-junction tunnel-FETs. Solid State Electron. 83:50–55
30. Singh S, Raj B (2020) Modeling and simulation analysis of SiGe heterojunction double gate vertical t-shaped tunnel FET. Superlattice. Microst. 142:106496
31. Jayaswal N, Raman A, Kumar N, Singh S (2019) Design and analysis of electrostatic-charge plasma based dopingless IGZO vertical nanowire FET for ammonia gas sensing. Superlattice. Microst. 125:256–270
32. Singh S, Khosla M, Wadhwa G, Raj B (2021) Design and analysis of double-gate junctionless vertical TFET for gas sensing applications. Appl. Phys. A 127(1):1–7
33. Kumar N, Raman A (2020) Prospective sensing applications of novel Heteromaterial based Dopingless nanowire-TFET at low operating voltage. IEEE Trans. Nanotechnol. 19:527–534

34. Hong Y, Kim C-H, Shin J, Kim KY, Kim JS, Hwang CS, Lee J-H (2016) Highly selective ZnO gas sensor based on MOSFET having a horizontal floating-gate. Sens. Actuators B Chem. 232:653–659
35. Shin W, Jung G, Hong S, Jeong Y, Park J, Jang D, Park B-G, Lee J-H (2020) Low frequency noise characteristics of resistor-and Si MOSFET-type gas sensors fabricated on the same Si wafer with In2O3 sensing layer. Sens. Actuators B Chem. 318:128087
36. Wadhera T, Kakkar D, Wadhwa G, Raj B (2019) Recent advances and progress in development of the field effect transistor biosensor: a review. J. Electron. Mater. 48(12):7635–7646
37. Chong C, Liu H, Wang S, Chen S (2021) Simulation and performance analysis of dielectric modulated dual source trench gate TFET biosensor. Nanoscale Res. Lett. 16(1):1–9
38. Madan J, Pandey R, Chaujar R (2020) Conducting polymer based gas sensor using PNIN-gate all around-tunnel FET. Silicon:1–9